`

Numerical Predictions of Transient Hydraulic Response of PWR Steam Generator Secondary Side to a Feedwater Pipe Break Using Flashing Flow Model

Jong Chull Jo
Korea Institute of Nuclear Safety, 62 Gwahak-ro, Yusung-gu, Daejeon, 34142, Korea
Corresponding author: jcjo@kins.re.kr

1. Introduction

For the structural integrity evaluation of a pressurized water reactor (PWR) steam generator (SG) performed in the process of design or licensing review, it is required to know the transient hydraulic loading on the SG tubes and other internal structures during blowdown following any of the two design basis accidents (DBAs) which are a feedwater line break (FWLB) and a main steam line break (MSLB).

Even though many experimental and numerical studies were performed to simulate the transient thermal-hydraulic responses of a PWR SG to either FWLBs or MSLBs [1-14], only few studies addressing multi-dimensional numerical simulations of the thermal-hydraulic responses to a sudden FWLB are found in the literature. Recently, Jo et al. [15] performed a numerical simulation of the transient flow field inside the secondary side of a PWR SG during blowdown following a FWLB. The non-flashing liquid flow through the broken feedwater pipe was assumed to evaluate the transient blowdown loading conservatively.

In this paper, CFD analyses of the transient flow field inside the SG secondary side of a PWR [16] during blowdown following a FWLB accident were performed for two different outlet boundary condition models of the flashing flow through the broken pipe. The prediction results for the two different outlet boundary condition models were compared with each other to examine their applicability to the practical regulatory confirmation calculations.

2. Analysis

2.1 Analysis Model

The PWR SG [16] considered in this paper (see Fig.1) is equipped with two economizer feedwater nozzles and one downcomer feedwater nozzle. During the normal SG full power operation, the economizer feedwater line supplies continuous feedwater flow to makeup 100 % of the SG's maximum steaming rate while the downcomer feedwater line accommodates 10 % of the total feedwater flow to the SG. It is assumed that a FWLB occurs at the weld point of either of the two economizer feedwater nozzles, which is located nearest to the SG during the full power operation.

Some investigators [17, 18] reported that, during the blowdown of a liquid at a very high pressure to the atmosphere through very short pipes, the highly pressurized subcooled liquid would discharge as a meta-stable liquid at a non-equilibrium state.

In addition, it was reported in references [19, 20] that the currently available two-phase critical flow models such as the Henry-Fauske model and the Moody model which have been widely employed in the reactor system design or safety analysis computer codes significantly underestimate the flowrates of saturated water through pipes with L/D ≤ 3 as compared to the measured data.

At present, neither general theoretical models for two-phase critical flow through the broad range outlet geometry nor numerical models for simulating the flashing flow of the meta-stable liquid jet experiencing breakup into droplets, evaporation, and expansion are available. Under such a situation, an effort to numerically simulate the SG hydraulic response to a FWLB as realistically as achievable was tried in this study by employing the thermal-phase change flashing flow model assuming the phase change of the compressed water into vapor by bulk boiling. Even this model is expected to result in underestimation of the critical flow rates because the effects of direct water jet discharge on the critical flowrate are not taken into account. The numerical model for thermal-phase change flashing flow was validated by Jo et al. [12].

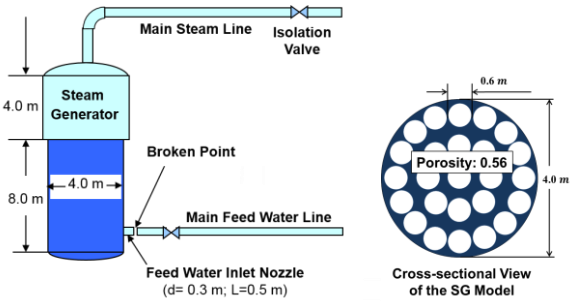

Fig.1 Simplified FWLB analysis model [15]

Governing equations

The same numerical analysis model as in reference [12] was chosen for calculating the transient three-dimensional turbulent flow in the PWR SG secondary side following the FWLB. The transport equations of velocity, pressure, temperature and turbulence were solved for the multi-phase fluid components using a commercial CFD code [21]. The flashing flow accompanying the thermal phase change was calculated by employing the inhomogeneous two-fluid model. The

`

turbulent viscosity was estimated by applying the $k-\omega$ based shear stress transport (SST) turbulence model [22]. The properties of the saturated vapor and liquid were retrieved from the database in the code [21].

Boundary and Initial Conditions

The upper and lower spaces of the SG were assumed to be initially occupied with saturated vapor and compressed water at a constant pressure of 7.5 MPa. The FWLB was assumed to occur at the weld point between the SG feedwater inlet nozzle and the feedwater supplying pipe in a very short time. This was modeled by defining a linear decrease in pressure from the initial state to the atmospheric pressure in 1.0 ms at the broken end of the feed water inlet nozzle. The main steam isolation valves of the SG were assumed to be closed instantly following the FWLB. The no-slip and adiabatic boundary conditions were specified to the solid wall surfaces. The water level $z_{w_i} = 8.0\ m$, and the initial velocity $U_i = 0.0\ m/s$ were given. The volumes of saturated steam and water were set to occupy each of the two layered spaces from top to bottom in the order of their density, respectively.

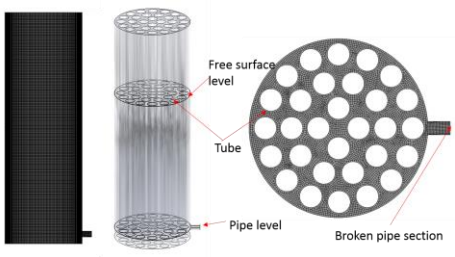

(a) Model 1

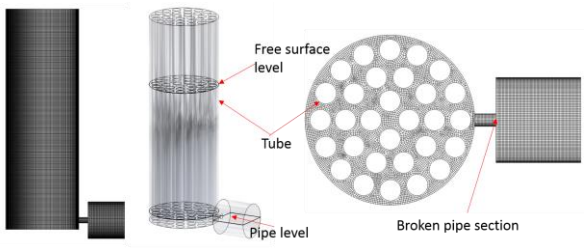

(b) Model 2

Fig. 2 Flashing flow analysis models

One of the two different outlet boundary condition models of the flashing flow through the broken pipe (Model 1) was modeled by limiting the numerical simulation domain to the broken pipe end cross-section to which the atmospheric pressure was specified after the pipe break, as shown in Fig. 2a. The other (Model 2) was modeled, as shown in Fig.2b, by extending the simulation domain to an atmospheric space surrounding the pipe broken end with the assumption that the space was initially maintained at the atmospheric pressure and the outer boundaries were constantly subjected to the atmospheric pressure during blowdown. Model 1 is simpler than Model 2 because of the simulation domain size.

2.2 Numerical Analysis

As shown in Fig.2, the whole calculation domains of the two analysis models including the SG, the inlet nozzle of the feed water pipe, and the outer ambient space of the broken pipe end (only for Model 2) were discretized into fine meshes of 1,440K and 1,800K sweep or tetra elements, respectively. Based on the result of the sensitivity study of an acceptable time step size for the present transient numerical calculations, time steps ranging from 0.001 ms to 0.01 ms were applied.

The analysis model at the steady-state condition was calculated for 0.01 seconds to obtain the initial pressure distribution in the model. An iterative computation for each time step was set to terminate when the maximum of the absolute sum of dimensionless residuals of governing equations became smaller than 0.0001.

The transient velocity and pressure of fluid were monitored at 6 different locations “Point 1~ Point 5” and the exit section as shown in Fig. 3. In the exit section, area averaged values of velocity and pressure were monitored.

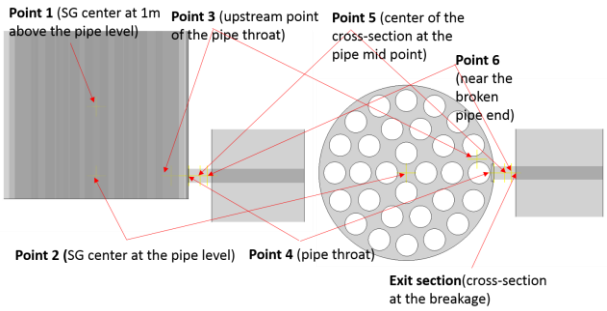

Fig. 3 Monitoring points

3. Results and Discussion

The numerical method applied to the present calculations was validated in the previous study [12].

Figures 4-6 show some typical calculation results of the transient fluid velocity and pressure responses to the FWLB for the two different outlet boundary condition models of the flashing flow through the broken pipe end.

Figure 4 displays the transient hydraulic contours around the broken pipe end at the elapsed times of 0.001 s and 0.1 s after the FWLB for the two boundary condition models. As shown in Fig.5, Model 2 seems to be able to simulate the thermal-hydraulic responses in the SG with the feedwater pipe to the FWLB more realistically than Model 1.

`

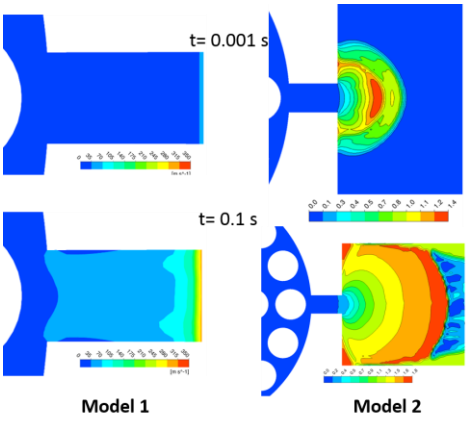

(a) Velocity contours

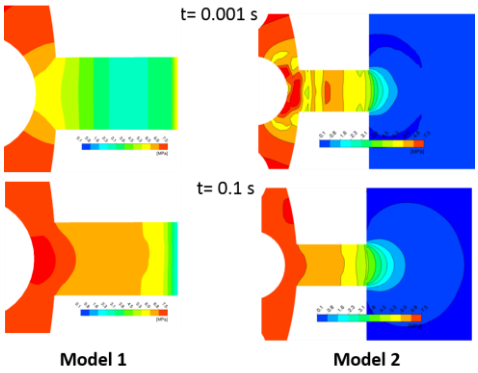

(b) Pressure contours

Fig. 4 Transient hydraulic responses at 0.001 s and 0.1 s

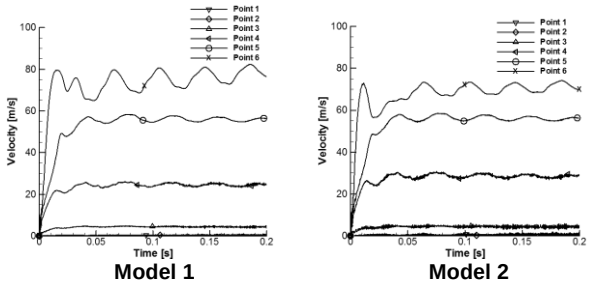

Fig. 5 Transient velocity responses at the 6 monitoring points

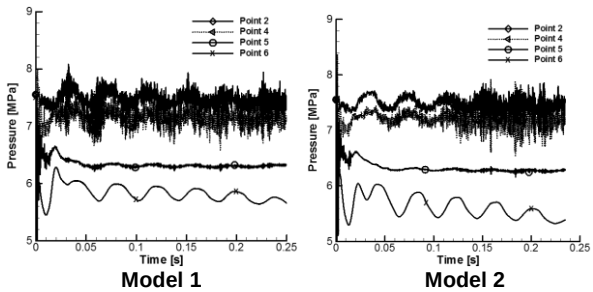

Fig. 6 Transient pressure responses at the 4 monitoring points

It is because Model 2 extends the calculation domain to include the flow field downstream the broken pipe end.

Figure 5 displays the transient velocity responses of the six different monitoring points during the early blowdown over the elapsed time of 0.2 s after the FWLB for the two boundary condition models. It is seen from Fig. 4 that Model 2 estimates the velocity at the feedwater nozzle outlet (the entrance to the SG) somewhat higher than Model 1 does while Model 2 estimates the velocity at the mid-point of the feedwater nozzle span somewhat lower than Model 1 does and the estimations inside the SG by the two models are similar.

Figure 6 shows the transient pressure responses of the four different monitoring points during the early blowdown over the elapsed time of 0.25 s after the FWLB for the two boundary condition models. As seen from Fig.6, Model 1 yields more fluctuating transient pressure disturbances during the early time period of blowdown over the elapsed time of 0.1 s because it assumes the step change in pressure at the broken pipe end at the beginning of blowdown in Model 1.

In general, the simulation results for both models are somewhat different from each other at the very beginning of blowdown and in the flow field near the broken pipe end. This is because the use of the outlet boundary condition model 2 results in a precise simulation of the flow field near the broken pipe end including particularly the ambient space downstream the blowdown exit. However, both models do not make any significant difference in their calculation results of the flow field inside the SG during the remaining blowdown period after the elapsed time of 0.1 s following the MFLB.

5. Conclusions

Based on the present CFD analysis results, it seems that both boundary condition models are generally acceptable for the application to the numerical prediction of the blowdown loading. However, it was confirmed that Model 2 extending the simulation domain to an atmospheric space surrounding the pipe broken end could yield more realistic simulation results of the present blowdown problem than the simpler Model 1 assuming a step pressure change at the broken pipe end.

REFERENCES

[1] Shier, W.G.; Levine, M.M., 1980, “PWR steamline break analysis assuming concurrent steam generator tube rupture,” ANS/ASME topical meeting on reactor thermal-hydraulics, 9 Oct 1980, Saratoga, NY, USA, Paper No. CONF-801002-9.

[2] Gallardo, S.; Querol, A.; Verdu, G., 2012, “Simulation of a main steam line break with steam generator tube rupture using trace,” Proceedings of the

`

PHYSOR 2012, 15~20 Apr 2012, Knoxville, TN, USA, American Nuclear Society, pp.2131-2144.

[3] Gallardo, S., Querol, A., and Verdú, G., 2014, "Improvements in the simulation of a main steam line break with steam generator tube rupture," Proceedings of the Joint International Conference on Supercomputing in Nuclear Applications + Monte Carlo, 27-31 October, 2013, Paris, France, Paper No. 05104.

[4] Kalra, S., and Adams, G., 1980, "Thermal Hydraulics of Steam Line Break Transients in Thermal Reactors—Simulation Experiments," ANS International Conference, American Nuclear Society, Washington, DC, Nov. 17–21, Vol. 35, Paper No. CONF-801107.

[5] Wolf, L., 1982, "Experimental results of coupled fluid-structure interactions during blowdown of the HDR-vessel and comparisons with pre- and post-test predictions," Nucl. Eng. Des., Vol. 70, No. 3, pp. 269~308.

[6] Saha, P., Ghosh, A., Das, T. K., and Ray, S., 1993, "Numerical simulation of pressure wave time history inside a steam generator in the event of Main Steam Line Break and Feedwater Line Break transients," Transient Phenomena in Nuclear Reactor Systems, ASME HTD-vol. 245/ NE-vol. 11, pp. 131-140

[7] Tinoco, H., 2002, "Three-dimensional modeling of a steam-line break in a boiling water reactor," Nucl. Sci. Eng., Vol. 140, No. 2, pp.152~164.

[8] Joo, H. G., Jeong, J.-J., Cho, B.-O., Lee, W. J., and Zee, S. Q., 2003, "Analysis of the OECD Main Steam Line Break Benchmark Problem Using the Refined Core Thermal-Hydraulic Nodalization Feature of the MARS/MASTER Code," Nucl. Technol., 142(2), pp. 166–179.

[9] Kang, K.H. et al., 2011, "Experimental Study on the Blowdown Load during the Steam Generator Feedwater Line Break Accident in the Evolutionary Pressurized Water Reactor," Annals of Nucl. Energy, Vol. 38, pp. 953-963.

[10] Hamouda, O., Weaver, D. S., and Riznic., 2015, Loading of Steam Generator Tubes during Main Steam Line Breaks, CNSC Contract No. 87055-11-0417 – R430.3, RSP-0305, Canadian Nuclear Safety Commission, Ottawa, Canada, pp. 1~171.

[11] Jo, J.C. and Moody, F.J., 2015, "Transient Thermal-Hydraulic Responses of the Nuclear Steam Generator Secondary Side to a Main Steam Line Break," ASME JPVT, Vol. 137, pp. 041301-1~7.

[12] Jo, J.C., Min, B.K., and Jeong, J.J., 2016, "Validation of a CFD Analysis Model for the Thermal-hydraulic Response of PWR Steam Generator to a Steam Line Break," ASME PVP 2016-63048, Proc. PVP 2016 Conf., July 17-21, Vancouver, BC, Canada.

[13] Hamouda, O., Weaver, D.S., and Riznic, J., 2016, "An Experimental Model Study of Steam Generator Tube Loading during a Sudden Depressurization," ASME JPVT, Vol. 138, pp. 041302-1~11.

[14] Jo, J.C. and Moody, F.J., 2016, "Effects of a Venturi Type Flow Restrictor on the Thermal-Hydraulic Response of the Secondary Side of a Pressurized Water Reactor Steam Generator to a Main Steam Line Break," ASME JPVT, Vol. 138, pp. 041304-1~12.

[15] Jo, J.C., Jeong, J.J., and Moody, F.J., 2016, "Transient Hydraulic Response of a PWR Steam Generator to a Feed Water Line Break Using the Non-Flashing Liquid Flow Model," ASME JPVT, accepted for publication.

[16] KHNP, 2011, APR+ Standard Safety Analysis Report, KHNP, Seoul, pp. 10.4-17.

[17] Weisman, J. and Tentner, A., 1978, "Models for Estimation of Critical Flow in Two-Phase Systems," Progress in Nuclear Energy, Vol. 2, pp. 183-197.

[18] Simones-Moreira, J.R., Vieira, M.M., and Angelo, E., 2002, "Highly Expanded Flashing Liquid Jets," J. Thermophysics and Heat Transfer, Vol. 16, No. 3, pp. 415-424.

[19] Ardron K.H. and Furness, R.A., 1976, "A Study of the Critical Flow Models Used in Reactor Blowdown Analysis," Nucl. Eng. Des., Vol. 39, pp. 257-266.

[20] Lien, P., 2016, "Scaling in Complex Thermal-Hydraulic Phenomena," ASME PVP2016-63047, Proc. PVP 2016 Conf., July 17-21, 2016, Vancouver, BC, Canada.

[21] ANSYS CFX User's Guide-14, ANSYS Inc., New York, 2012.

[22] Menter, F. R., 1994, "Two Equation Eddy-Viscosity Turbulence Models for Engineering Applications," AIAA J., 32(8), pp. 1598-1604.